Bayesian Estimation of European Sulphur Emissions Using Monitoring Data and an Acid Deposition Model

GUDMUND HØST[1]

Abstract

A statistical method for estimating national emissions of acidifying air pollutants in Europe is presented. The method uses an acid deposition model to match official emissions data from European countries and measured depositions from a monitoring network. An application to 1990 sulphate data demonstrates the method and suggests some tendencies in the reported emissions. The proposed framework may prove useful for verifying national compliance with emissions standards, and the method should be applicable also to other substances than sulphur dioxide. The problem of designing an optimal monitoring network may also be assessed within the proposed statistical framework.

KEY WORDS: Sulphate deposition; Source allocation; EMEP-model; Maximum posterior density; Cross-validation; Bayesian Kriging.

[1]Norwegian Computing Center, Box 114 Blindern, 0314 Oslo, Norway.

1 Introduction

The Convention on Long-Range Transboundary Air Pollution was adopted in Geneva in 1979. This is an international agreement with the objective of protecting man and his environment against air pollution including long-range transboundary air pollution. In particular, various protocols to the Convention have put explicit obligations on the participating nations pertaining to control and reduction of emissions. A protocol on the reduction of sulphur emissions or their transboundary fluxes by at least 30% was adopted in Helsinki in 1985. Related protocols on nitrogen oxides and volatile organic compounds were adopted in 1988 and 1991. In addition, a second sulphur protocol on further reduction of sulphur emissions was adopted in Oslo in 1994. Rather than proportional reduction of sulphur emissions, this protocol calls for cost-effective reductions to minimize the effects on the environment. Of particular relevance to this paper is the emphasis of the Oslo Protocol on review of the information supplied by the parties. Indeed, the Oslo Protocol establishes a committee to review compliance by the countries with their obligations to reduce sulphur emissions.

The purpose of this paper is to introduce a statistical framework for monitoring compliance by European countries with their obligations to reduce air pollutant emissions. The method is illustrated by an application to sulphur data from 1990.

In our example, we use concentrations of sulphate in precipitation from the EMEP monitoring network in 1990 (Pedersen, Schaug and Skjelmoen 1992). We also use national sulphur emissions reported to the Geneva Convention, as given in Barrett et al (1995). In our approach, the reported sulphur emission from each country characterizes a probability distribution and the true emission is a random variable drawn from this distribution. The reported emissions are linked to the monitored depositions by using the acid deposition model developed by the Meteorological Synthesizing Centre - West (MSC-W) of EMEP, located at the Norwegian Meteorological Institute. This model is described in various publications. Its latest implementation and further references are given in Barrett et al (1995). Coefficients from the acid deposition model describe the transfer of emitted sulphur dioxide from countries to wet deposited sulphate at monitoring stations. These transfer coefficients are used as regressors in a spatial linear regression model with the measured depositions as response and the emissions as regression coefficients. Using a Bayesian framework (Box and Tiao 1973; Berger 1985), we obtain a statistical method for combining the various sources of information.

Within the context of spatial prediction, a Bayesian framework is described in Kitanidis (1986), Omre (1987), and Omre and Halvorsen (1989). Some extensions are given in Handcock and Stein (1993) and Hjort and Omre (1994).

The results given in this paper for sulphur emissions may be further improved upon by including other components, such as measured sulphur dioxide and particulate sulphate, in the statistical model. For future assessment of national reductions of sulphur emissions, we also recommend combining data from subsequent years.

The statistical model presented here may have wide applications to other fields of environmental modeling, such as oceanography and hydrology. For example, if we have field data on marine pollutants and initial (prior) estimates of pollutant sources, then a statistical model may use an oceanographic transport model to obtain (posterior) estimates of pollutant sources. Alternatively, we may have prior estimates of pollutant sources in a river system and a network of stations monitoring river pollutants. Again, a statistical model and a physical model may provide a unique framework for integrating emissions information and monitoring data. Such a unified framework may also provide a basis for improving the physical model.

Although the focus here is on estimation of input variables (emissions), our model may also be used for enhancing the prediction of output variables (depositions). This will be done in Section 5.3, where we apply the statistical model to spatial prediction of sulphate deposition. Finally, our results are also relevant for prediction of critical load exceedances.

Our paper is structured as follows. The data are presented in Section 2. In Section 3, the statistical framework is introduced. The method of parameter estimation is described in Section 4 and some special cases are discussed. The application to European sulphur emissions is described in Section 5. A discussion of our results and suggestions for further work are given in Section 6.

2 Data and Available Information

In the analysis 48 national and regional emissions from 1990 are used, as presented in Barrett, Seland, S., Sandnes, Styve & Tarrasón (1995). These sulphur dioxide emissions will be referred to as *prior emissions*, and their values are given in Table 1 (left column). Of these prior emissions, 30 values are officially submitted. The remaining 18 values are estimated by MSC-W through various other external data.

The deposition data are yearly averages of sulphate in precipitation measured at 42 locations in Europe, obtained by averaging daily values from the EMEP monitoring network (Schaug, Pedersen & Skjelmoen 1992) throughout 1990. For each location, the data value is a weighted average of sulphate concentrations, with the weights taken as the proportion of daily to total 1990 precipitation at the location. Stations with more than 10% missing data in any month have been excluded from the analysis. The sulphate data are further described in Schaug, Pedersen, Skjelmoen & Kvalvågnes (1992).

The acid deposition model of MSC-W (Barrett et al. 1995) was used to obtain transfer coefficients from emitted sulphur dioxide to wet deposited sulphate. We will refer to this acid deposition model as the *EMEP model*. Each transfer coefficient describes the contribution from a unit emission in a specific country (or region) to the sulphate concentration at a specific monitoring station.

The EMEP model quantifies current knowledge of atmospheric transport, chemical transformations and deposition processes, and it is the explanatory tool linking emissions to monitoring data.

While the monitoring data are spatial point values, the sulphate predictions from the EMEP model are spatial averages over 150 km $\times$ 150 km grid blocks. Particular attention must be given to monitoring stations near large emission sources, because the EMEP model is not designed to describe local deposition phenomena. Therefore, including monitoring stations near large sources may amplify the variance in emission estimates. On the other hand, the monitoring data are often not sensitive to local emissions, because the EMEP monitoring stations are located to measure background concentrations. Consequently, a monitoring station located in a grid block with large local emissions is likely to measure a sulphate concentration which is lower than the true grid-block average. This effect may introduce systematic errors and would give biased emission estimates.

To take proper care of local deposition phenomena, we would need a much more elaborate statistical model than we have used here. Since our present model is Gaussian, we have instead applied a reasonable data screening procedure. The criterion used here was to delete stations in grid blocks with yearly emissions exceeding 10 tons of sulphur per square km. One British station and five stations in central Europe were removed by this criterion. In

addition, one station on Faeroe Islands was removed due to sea spray contamination. The resulting set of 42 monitoring stations is shown in Figure 1.

[Figure 1 here]

Figure 2 shows the EMEP predicted sulphate concentrations (using reported emissions) versus the measured concentrations for 1990 after the data screening described above. We see that the EMEP predicted concentrations are mostly smaller than the measured concentrations. Also, there seems to be no indications of heteroscedasity in these data.

[Figure 2 here]

The method we shall propose requires a prior estimate for the uncertainty in the reported emissions. We have used a prior coefficient of variation $\gamma_0 = 0.3$, based on recommendations from MSC-W. This reflects the view that reported emissions have a standard deviation of 0.3 times the reported value. The sensitivity of our results to this parameter is discussed in Sections 5 and 6.

3 Statistical Model

Consider a random field $y(\boldsymbol{x})$, where $\boldsymbol{x}$ is the location within some geographic region. Let $y(\boldsymbol{x})$ have the decomposition

$$y(\boldsymbol{x}) = \boldsymbol{b}'(\boldsymbol{x})\boldsymbol{\beta} + \epsilon(\boldsymbol{x}). \tag{1}$$

Here, $\boldsymbol{b}(\boldsymbol{x})$ is an m-vector of known functions and $\boldsymbol{\beta}$ is an m-vector of parameters to be estimated. Furthermore, $\epsilon(\boldsymbol{x})$ is a Gaussian random field with zero mean and covariance

$$\text{Cov } \{y(\boldsymbol{x}_1), y(\boldsymbol{x}_2)\} = \sigma^2 \, \rho(\|\boldsymbol{x}_1 - \boldsymbol{x}_2\|; a).$$

Here, σ^2 is the variance of the residual process, a is a "range" parameter. and $\rho(\cdot; a)$ is a correlation function to be fitted to data. The focus of this paper is on estimation of $\boldsymbol{\beta}$, but the unknown parameters σ^2 and a must also be estimated.

In our application, $y(\boldsymbol{x})$ represents the (true) sulphate concentration at location $\boldsymbol{x}$. Furthermore, $b_j(\boldsymbol{x})$ represents the contribution to this concentration as predicted by the EMEP model for a unit emission of sulphur dioxide from country j; $j = 1, \ldots, m$. The unknown emission from country j is β_j, so $\boldsymbol{b}'(\boldsymbol{x})\,\boldsymbol{\beta}$ is the sulphate concentration predicted by the EMEP model. For

$\boldsymbol{\beta} = \mathbf{0}$ the EMEP model predicts zero sulphate concentration at all locations throughout Europe, because the model accounts for emissions from all possible contributors to European air pollution. Differences between the true sulphate concentrations and the concentrations predicted by the EMEP model are absorbed into the residual field $\epsilon(\boldsymbol{x})$. If the EMEP-model is reasonable for predicting large concentations of yearly sulphate averages, then the Gaussian model for $\epsilon(\boldsymbol{x})$ may be adequate. As seen from Figure 2, there are no indications that a data transformation is neccessary in the present application.

We introduce a *Bayesian* framework (Berger 1985), and use *prior* and *posterior* to denote knowledge of $\boldsymbol{\beta}$ without and with observations of the y–field. Bayesian approaches to spatial prediction and spatial parameter estimation have been developed by Kitanidis (1986), Omre (1987), Pilz (1991) and Le & Zidek (1992). However, the use of Bayesian methods to combine information from deterministic models with data is less common. Therefore, some details of the Bayesian approach will be given in the folowing. A priori, we assume independence, and take each β_j to be a normally distributed random variable with prior mean β_{0j} and prior coefficient of variation γ_0. Hence, the prior probability distribution of $\boldsymbol{\beta}$ is

$$\boldsymbol{\beta} \sim N\left(\begin{pmatrix}\beta_{01}\\ \vdots \\ \beta_{0m}\end{pmatrix}, \gamma_0^2 \begin{pmatrix}\beta_{01}^2 & & 0 \\ & \ddots & \\ 0 & & \beta_{0m}^2\end{pmatrix}\right). \tag{2}$$

Here, we take the prior mean $\boldsymbol{\beta}_0 = (\beta_{01}, \ldots, \beta_{0m})'$ to be the vector of reported emissions from each country. The model for prior variance signifies that large reported emissions are likely to be more uncertain than small emissions. Without observations of the y-field, the natural "estimate" of $\boldsymbol{\beta}$ is $\boldsymbol{\beta}_0$, i.e. the reported emissions. The diagonal structure of the prior variance for $\boldsymbol{\beta}$ is not crucial for our analysis. In particular, prior knowledge of dependencies between emissions from different regions may easily be included in the prior distribution (2). The emissions $\boldsymbol{\beta}_0$ are obtained through national statistics for fuel consumption and industrial activity, and through the use of various "emission factors" on industry and vehicles. Uncertainty in such emission factors may as a first approach be taken as constant, giving the constant coefficient of variation parametrization used here. Alternative models should be investigated in the future. The prior coefficient of variation γ_0 must be specified from expert knowledge. Alternatively, we could extend our model by putting a hyperprior on γ_0 and try to estimate this parameter from data.

The motivation for regarding $\boldsymbol{b}(\boldsymbol{x})$ as fixed and $\boldsymbol{\beta}$ as random is the assumption that the reported emissions are much more uncertain than the EMEP

model. In practice, there may be some uncertainty in the EMEP model due to estimation of physical and chemical parameters. In our statistical framework, such possible uncertainty in the EMEP model would be interpreted as uncertainty in the reported emissions.

Since we have no a priori knowledge about the variance parameter σ^2, we use the commonly used non-informative prior $p(\sigma^2) \propto \sigma^{-2}$. For the range parameter a, we use the prior $p(a) = (1+a)^{-2}$, as suggested by Handcock and Wallis (1994). The prior chosen for a reflects that the residual field ϵ should capture high-frequency fluctuations, hence a short range is more likely a priori than a long range. The interested reader is referred to Berger (1985) for an introduction to Bayesian statistics and discussions on how to choose prior densities.

Let $\boldsymbol{y} = (y(\boldsymbol{x}_1), \ldots, y(\boldsymbol{x}_n))'$ be the data vector of n measurements of sulphate. The information in the data are contained in the likelihood

$$L(\boldsymbol{\beta}, \sigma^2, a; \boldsymbol{y}) = |2\pi \boldsymbol{R}_a|^{-1/2} \sigma^{-n} \exp\left\{ -\frac{1}{2\sigma^2} [\boldsymbol{y} - \boldsymbol{B}\boldsymbol{\beta}]' \boldsymbol{R}_a^{-1} [\boldsymbol{y} - \boldsymbol{B}\boldsymbol{\beta}] \right\}. \quad (3)$$

Here, the j'th column of $\boldsymbol{B}$ is $b_j(\cdot)$ evaluated at the data locations $\{\boldsymbol{x}_1, \ldots, \boldsymbol{x}_n\}$. Furthermore, the (i,j)'th element of the correlation matrix $\boldsymbol{R}_a$ is $\rho(\|\boldsymbol{x}_i - \boldsymbol{x}_j\|; a)$.

From Bayes' theorem, the posterior density of $(\boldsymbol{\beta}, \sigma^2, a)$ is

$$p(\boldsymbol{\beta}, \sigma^2, a|\boldsymbol{y}) \quad \propto \quad p(\sigma^2)\; p(a)\; p(\boldsymbol{\beta}; \boldsymbol{\beta}_0, \gamma_0^2)\; L(\boldsymbol{\beta}, \sigma^2, a; \boldsymbol{y}).$$

Inserting the appropriate expressions for the prior and the likelihood, we get

$$\begin{aligned} p(\boldsymbol{\beta}, \sigma^2, a|\boldsymbol{y}) \quad \propto \quad & \frac{1}{\sigma^{n+2}} \frac{1}{(1+a)^2} \, |\gamma_0^2 \, \mathrm{diag}(\boldsymbol{\beta}_0 \boldsymbol{\beta}_0')|^{-1/2} \\ & \times \exp\left\{ -\frac{1}{2} (\boldsymbol{\beta} - \boldsymbol{\beta}_0)' [\gamma_0^2 \, \mathrm{diag}(\boldsymbol{\beta}_0 \boldsymbol{\beta}_0')]^{-1} (\boldsymbol{\beta} - \boldsymbol{\beta}_0) \right\} \\ & \times |\boldsymbol{R}_a|^{-1/2} \exp\left\{ -\frac{1}{2\sigma^2} [\boldsymbol{y} - \boldsymbol{B}\boldsymbol{\beta}]' \boldsymbol{R}_a^{-1} [\boldsymbol{y} - \boldsymbol{B}\boldsymbol{\beta}] \right\}. \end{aligned} \tag{4}$$

This posterior can be extended to $p(\boldsymbol{\beta}, \sigma^2, a, \gamma_0|\boldsymbol{y})$ in order to include uncertainty in γ_0. The right hand side of (4) will need to be multiplied by an appropriate hyperprior $p(\gamma_0)$.

4 Parameter Estimation

According to the Bayesian paradigm, inference about $\boldsymbol{\beta}$, σ^2 and a should be based on the posterior density (4). In the present application, we have $m + 2 = 50$ parameters and $n = 42$ observations. Therefore, the parameters can not be estimated by standard frequentist methods. In contrast, the Bayesian framework allows for coherent parameter estimation by including prior information.

The most common Bayes estimate is the mean of the posterior distribution, while other Bayes estimates include the posterior median and the posterior mode. In the present application, we have used the posterior mode, which is related to the maximum likelihood estimate. The posterior mode can be interpreted as the "most likely" parameter value, given the prior and the data. In the sense of minimum posterior expected loss, the posterior mean is optimal under a qudratic loss function, while the posterior mode is optimal under the somewhat special "0-1" loss function (Berger 1985, pp. 161–163). Certainly, the mean, median and mode are identical when the posterior distribution is multivariate Gaussian. Hence, the posterior mode can be regarded as a normal approximation to the posterior mean.

The posterior mode is often fast to calculate, although some posterior densities can be hard to maximize. On the other hand, calculation of the posterior

mean (or median) involves integrating the posterior, which can be computationally slow. Nevertheless, faster computers make Markov Chain Monte Carlo (MCMC) methods (Tanner 1993; Gilks, Richardson and Spiegelhalter 1996) increasingly competetive for assessment of the posterior distribution. Therefore, MCMC methods should be considered in future applications to emissions estimation.

Maximizing the log posterior amounts to maximizing the log-likelihood function with an additional regularization term. Since the posterior density is just a penalized likelihood function, we may apply a modified method of numerical maximum likelihood estimation for computation of the posterior mode. We use the scoring method, which was introduced for spatial data by Mardia and Marshall (1984). Some caution should be exercised when selecting the covariance function to avoid multimodality, see Warnes and Ripley (1987), and the rejoinder of Mardia and Watkins (1989). Denote the posterior mode parameter estimate by $(\widehat{\boldsymbol{\beta}},\widehat{\sigma^2},\widehat{a})$. An estimate of the covariance matrix of the posterior mode may be obtained by inverting the Hessian of $\log p(\boldsymbol{\beta}, \sigma^2, a|y)$. We get

$$\widehat{\mathrm{Var}}\{(\widehat{\boldsymbol{\beta}}', \widehat{\sigma^2}, \widehat{a})\} = -\left[\mathrm{E}\frac{\partial^2 \log p(\boldsymbol{\beta}, \sigma^2, a|\boldsymbol{y})}{\partial(\boldsymbol{\beta}', \sigma^2, a)^2}\right]^{-1}_{(\beta,\sigma^2,a)=(\widehat{\beta},\widehat{\sigma^2},\widehat{a})}. \qquad (5)$$

The right hand side of (5) would be the exact posterior parameter covari-

ance matrix if the posterior had been multivariate normal in $(\boldsymbol{\beta}, \sigma^2, a)$. Thus the estimate (5) is a normal approximation to the posterior covariance matrix. Similar approaches to summarizing the posterior (mode and Hessian) are taken in the use of the EM-algorithm, see Dempster, Laird & Rubin (1977) and Louis (1982). Since the estimate is based on the logarithm of the posterior, we do not need to know the normalizing constant in (4).

Some special cases will be illustrated by fixing σ^2 and a. Linear algebra shows that the conditional distribution of the emissions $\boldsymbol{\beta}|\sigma^2, a$ is multivariate normal with first and second moments

$$\begin{aligned} \mathrm{E}\{\boldsymbol{\beta}|\sigma^2, a\} &= (\boldsymbol{\Sigma}_0^{-1} + \sigma^{-2}\boldsymbol{B}'\boldsymbol{R}_a^{-1}\boldsymbol{B})^{-1}(\boldsymbol{\Sigma}_0^{-1}\boldsymbol{\beta}_0 + \sigma^{-2}\boldsymbol{B}'\boldsymbol{R}_a^{-1}\boldsymbol{y}), \quad (6) \\ \mathrm{Var}\{\boldsymbol{\beta}|\sigma^2, a\} &= (\boldsymbol{\Sigma}_0^{-1} + \sigma^{-2}\boldsymbol{B}'\boldsymbol{R}_a^{-1}\boldsymbol{B})^{-1}, \quad (7) \end{aligned}$$

where $\boldsymbol{\Sigma}_0 = \gamma_0^2 \,\mathrm{diag}(\boldsymbol{\beta}_0\boldsymbol{\beta}_0')$. Thus, the conditional mode $\widehat{\beta}|\sigma^2, a$ is equal to the right hand side of (6), with variance Var $\{\widehat{\beta}|\sigma^2, a\}$ given by (7).

Formulae (6)–(7) are discussed in the following remarks.

1. Let $\gamma_0 \to \infty$ and $n \geq m$. This represents a situation with many monitoring stations and no prior information on emissions. Then

$$\widehat{\boldsymbol{\beta}}|\sigma^2, a \;\to\; (\boldsymbol{B}'\boldsymbol{R}_a^{-1}\boldsymbol{B})^{-1}\boldsymbol{B}'\boldsymbol{R}_a^{-1}\boldsymbol{y}$$

$$\text{Var}\ \{\widehat{\boldsymbol{\beta}}|\sigma^2, a\} \quad \rightarrow \quad \sigma^2(\boldsymbol{B}'\boldsymbol{R}_a^{-1}\boldsymbol{B})^{-1},$$

which is the maximum profile likelihood estimate of $\boldsymbol{\beta}$. When σ^2 and $\boldsymbol{R}_a$ are known, this is equivalent to the generalized least squares estimate. Furthermore, inserting $\boldsymbol{R}_a = \boldsymbol{I}$, we get the ordinary least squares estimate.

2. Let $\gamma_0 \rightarrow 0$. Then $\widehat{\boldsymbol{\beta}}|\sigma^2, a \rightarrow \boldsymbol{\beta}_0$ and Var $\{\widehat{\boldsymbol{\beta}}|\sigma^2, a\} \rightarrow \boldsymbol{\Sigma}_0$. This is just the mean and variance of the prior density, which is data-independent. Thus, with exact emission reports, there is no need to consider the monitoring data.

3. Formula (6) represents the general situation with γ_0 finite and positive. Then we may estimate $\boldsymbol{\beta}$ also for $n < m$, and the emission estimates will be a weighted combination of the prior emission and the maximum likelihood estimate.

4. A measure of the total variance in estimating $\boldsymbol{\beta}|\sigma^2, a$ is tr(Var $\widehat{\boldsymbol{\beta}}|\sigma^2, a$). Since $\boldsymbol{B}'\boldsymbol{R}_a^{-1}\boldsymbol{B}$ is a positive definite matrix, it follows from (7) that the total variance is minimized for some positive finite value of γ_0 when σ^2 and a are fixed. Thus, better emission estimates (smaller total variance) are obtained by using both prior information and data than by using either of these sources of information separately.

5 Results

5.1 Main Results

A correlation function must be specified prior to parameter estimation. The fit of any particular choice of correlation function should be checked visually, because it may be difficult to choose between correlation functions automatically. We found a reasonable fit using the exponential correlation function $\rho(h;,a) = \exp(-3h/a)$. Here, the correlation range a is the distance beyond which correlation is less than 0.05. The factor 3 in the exponent is introduced to make the range parameter a comparable with alternative correlation functions, in accordance with the geostatistical literature. Figure 3 shows the empirical correlogram and the estimated correlation function. The *correlogram* is the average covariance between station pairs at a specified lag divided by the overall variance. Since both the correlogram and the fitted correlation function tend to one as the lag tends to zero, there are no indications of measurement error effects in the sulphate data. This is partly because the sulphate data used in this analysis are averages over many values (i.e. one year of daily observations), but also because removal of stations near large emission sources may reduce short-range variability in the fitted residuals.

[Figure 3 here]

The maximum posterior density algorithm gave residual standard deviation estimate $\widehat{\sigma} = 0.29\, mg(S)/l$ and correlation range estimate $\widehat{a} = 851\, km$. This suggests that sulphate residuals will be virtually uncorrelated for lags greater than $851\, km$. The estimated standard error of the estimated residual standard deviation and of the correlation range were $0.15\ mg(S)/l$ and $300\, km$, respectively.

The results for the estimated emissions are described in Figure 4 and in Table 1. In Figure 4, the reported emissions and the estimated emissions are shown. The upper and lower boundaries of the boxes indicate 63% confidence intervals for the emissions ($\pm$ one standard deviation), while the central bars are the reported (broken line) or estimated (full line) emissions. Figure 4 shows that the estimation method gives larger emissions for Italy and United Kingdom than reported. For Italy, United Kingdom and Poland, the heights of the full boxes in Figure 4 are smaller than the heights of the broken boxes. For these countries, the estimated emissions have smaller estimated posterior than prior uncertainty. Moreover, Figure 4 shows smaller estimated emissions than reported for former German Democratic Republic and Poland.

[Figure 4 here]

Table 1 shows that our method of including information from the EMEP model and sulphate measurements allocate an additional 464 000 tons of

sulphur dioxide to Italy (21% increase) and an additional of 446 000 tons to United Kingdom (12% increase), as compared to the reported emissions. Similarly, our method indicates that emissions from former German Democratic Republic were 210 000 tons smaller than reported and emissions from Poland were 99 000 tons smaller than reported, corresponding to 3–4% of the respective reported emissions. The estimation method suggests that the total emissions of sulphur dioxide from all European sources were 912 000 tons greater (2%) than reported. A total of 32 estimated emissions exceeded the prior emissions, while 4 estimates were smaller than reported. For 12 regions the estimated and reported emissions were equal.

[Table 1 here]

Our method also gives estimated correlation between posterior estimated emissions from different countries. All these estimated correlations were smaller than ± 0.3.

Table 2 shows the EMEP predicted sulphate concentrations at the monitoring locations using the estimated emissions instead of the reported emissions. Only 6 locations get slightly smaller concentrations than the prior predictions. Some regions of largest increase seem to be former Yugoslavia and Norway. These results are only indicative for the updated deposition situation in Europe, because the density of monitoring stations vary geographi-

cally. To obtain a complete picture, we would have to evaluate the EMEP model for all grid blocks in Europe, not only for the monitoring stations.

[Table 2 here]

5.2 Sensitivity Study

The sensitivity of the statistical model was checked through analysis of the results from various model assumptions. We were particularly interested in the capability of the method to detect unusual prior emissions. In addition, we investigated the sensitivity to prior uncertainty. We reestimated the emissions for prior coefficient of variation $\gamma_0 = \{0.2, 0.3, 0.5, 1.0\}$. Furthermore, we varied the prior emission of the greatest contributor, former German Democratic Republic (DD). The hypothetical prior emissions chosen for DD were the official emission (4 755 000 tons) multiplied by factors 0.5, 1.0 and 2.0.

The results are shown in Table 3 for German Democratic Republic (DD), United Kingdom (GB), Italy (IT) and Poland (PL). The three latter countries were selected because they are important contributors, whose emissions can be estimated with relatively good precision (small posterior coefficient of variation). The first column of Table 3 represents the reported emissions ($\gamma_0 = 0$). Wee see (Table 3, upper panel) that when the DD prior emission is

unreasonable small, both the DD and PL posterior emissions are increased compared to the prior emissions. Correspondingly, Table 3 (lower panel) shows that when the DD prior emission is unreasonably large, both the DD and PL emissions are reduced a posteriori. Therefore, it seems that the DD and PL emissions may be confounded in our statistical model. Possibly, a different configuration of the monitoring network could give better separation of the emissions from these two regions. On the other hand, it is possible that we may need higher resolution in the EMEP model to separate these regional emissions.

The middle panel of Table 3 shows the posterior emissions for varying values of γ_0 when the DD prior emission is as reported. We see that the sensitivity to γ_0 is quite different for the various national posterior emissions. Changing γ_0 from 0 to 1 has a small effect on DD and PL posterior emissions and a large effect on GB and IT posterior emissions. Hence, it seems important to try to estimate γ_0 in future applications.

When interpreting the columns of Table 3, recall that the posterior variability will increase when the hypothetical DD prior emission increases. Therefore, for a fixed prior coefficient of variation, the IT, PL and GB posterior emissions will tend to be closer to their reported values when the hypothetical DD emission is small (upper panel) than when the hypothetical DD emission is large (lower panel).

Across all three panels of Table 3, we see that the emissions from IT and GB are increased a posteriori. In particular, Table 3 (middle panel, right column) gives the posterior emissions for the reported DD prior emissions when the deposition data are given much weight. We see that the deposition data suggest a small posterior decrease of DD and PL emissions, and a substantial posterior increase of the GB and IT emissions. However, to obtain significant results, we would need more monitoring data.

5.3 Cross-validation of sulphate values

While we described emissions estimation in the previous sections, we now focus on implications for prediction of sulphate concentrations. We will do this by introducing a statistical interpolator, and compare the predictive capability of the EMEP model predictor with this interpolator.

For a given location $\boldsymbol{x}$, the sulphate value can be inferred from the interpolator

$$\widehat{y}(\boldsymbol{x}) = \boldsymbol{b}'(\boldsymbol{x})\widehat{\boldsymbol{\beta}} + \boldsymbol{r}'(\boldsymbol{x})\boldsymbol{R}_{\widehat{a}}^{-1}(\boldsymbol{y} - \boldsymbol{B}\widehat{\boldsymbol{\beta}}). \tag{8}$$

Here, the elements of the n-vector $\boldsymbol{r}(\boldsymbol{x})$ are $(\boldsymbol{r}(\boldsymbol{x}))_i = \rho(\|\boldsymbol{x} - \boldsymbol{x}_i\|; \widehat{a})$. For given covariance parameters the interpolator (8) corresponds to the Bayesian Kriging interpolator described by Omre (1987) and Omre and Halvorsen

(1989). The term $\boldsymbol{b}'(\boldsymbol{x})\widehat{\boldsymbol{\beta}}$ on the right hand side of (8) can be interpreted as the EMEP prediction based on estimated emissions. The second term on the right hand side of (8) interpolates the fitted residuals $(\boldsymbol{y} - \boldsymbol{B}\widehat{\boldsymbol{\beta}})$. This term represents deviations between the observed and predicted sulphate concentrations. By replacing $\widehat{\boldsymbol{\beta}}$ in equation (8) with the right hand side of (6) the interpolator may be expressed

$$\widehat{y}(\boldsymbol{x}) = \boldsymbol{\alpha}'\,\boldsymbol{y}.$$

Here the weights $\boldsymbol{\alpha}$ are

$$\boldsymbol{\alpha} \;=\; \boldsymbol{R}_{\hat{a}}^{-1}\boldsymbol{r}(\boldsymbol{x}) \;+\; \boldsymbol{R}_{\hat{a}}^{-1}\boldsymbol{B}(\widehat{\sigma^2}\boldsymbol{\Sigma}_0^{-1} + \boldsymbol{B}'\boldsymbol{R}_{\hat{a}}^{-1}\boldsymbol{B})^{-1}[\boldsymbol{b}(\boldsymbol{x}) - \boldsymbol{B}'\boldsymbol{R}_{\hat{a}}^{-1}\boldsymbol{r}(\boldsymbol{x})].$$

The corresponding interpolation error estimate is the usual

$$\text{Var}\,\{y(\boldsymbol{x}) - \widehat{y}(\boldsymbol{x})\} = \widehat{\sigma^2}(\boldsymbol{\alpha}'\boldsymbol{R}_{\hat{a}}\boldsymbol{\alpha} - 2\,\boldsymbol{\alpha}'\boldsymbol{r}(\boldsymbol{x}) + 1). \tag{9}$$

After estimating the parameters, the following cross-validation exercise was carried out. One monitoring station at a time was omitted and that location was interpolated using all other data. The procedure was repeated for each of the 42 monitoring stations. Then the cross-validated (interpolated) sulphate values were compared with the observed sulphate values.

Figure 5 shows observed and cross-validated sulphate concentrations. Compared to Figure 2, there seems to be smaller bias in the interpolated sulphate

values. For each location, we form the squared difference between the measured sulphate value and the interpolated (cross-validated) value. Denote the root mean of all such values as the *RMS true interpolation error*. In this paper, we have used the arithmetic mean, although one could alternatively use a spatially weighted mean. The cross-validation exercise also gives an estimate of the interpolation variance at each location, as given by (9). Denote the root mean of all such values as the *RMS estimated interpolation error*. The RMS true interpolation error is 0.227 and the RMS estimated interpolation error is 0.235. This close correspondence between estimated and true interpolation errors indicates that the proposed statistical model is a reasonable method for assessing sulphate concentrations in Europe.

[Figure 5 here]

In comparison, we can also calculate the *RMS prediction error* from the squared differences between measured sulphate values and the values predicted by the EMEP model (i.e., not interpolating the residual). The RMS prior prediction error (using reported emissions only) is 0.334, while the RMS posterior prediction error is 0.318. Thus, there is only a slight improvement on sulphate predictive capability by incorporating the monitoring data, as long as we do not interpolate the residuals. This is because much weight is given to the prior emissions in the present example. A larger prior coefficient of variation would give smaller posterior prediction errors. For example, us-

ing $\gamma_0 = 0.5$ reduces the RMS posterior prediction error to 0.288. Prediction performance may also be improved by including more data, either from other years or from other monitored components.

The results of this section indicate that prediction performance may be further improved by also interpolating the residual field. Although this may be preferable in terms of predicting actual sulphate concentrations, it will reduce interpretability, since unexplained variability would be introduced into the predictor. This unexplained variability represents sulphur that cannot be accounted for in the mass–balance formulation of the EMEP model.

The results of this section should be interpreted with some care, since we are in fact assessing the quality of interpolation and prediction of sulphate, not emission estimates. Also, there may be some dispute as to how one should average the cross-validated and predicted values. In particular, we may want to give greater weight to distant locations, since these locations "represent" a larger area than locations from densely sampled regions.

6 Discussion

We have proposed a statistical framework for combining reported emissions, monitored deposition data and information from an acid deposition model. Our method was used to investigate sulphur emissions and sulphur wet depositions in Europe during 1990 with the view towards improving the emissions estimates.

The precision of our results depends on the prior uncertainty about reported emissions. The prior uncertainty is quantified by the hyperparameter γ_0, which has to be specified prior to the analysis. In the absence of exact knowledge of γ_0, the following considerations apply. Choosing γ_0 too small will overemphasize the confidence in reported emissions and give emissions estimates that are close to the reported emissions. On the other hand, choosing γ_0 too large will underemphasize emission reports and the resulting emissions estimates will be based mainly on sulphate data and the EMEP acid deposition model. This will give less biased emissions estimates, but greater posterior variance. Thus, a pragmatic point of view is to regard γ_0 as a smoothing parameter governing the bias-variance trade-off. If the main concern is to identify potentially unreliable emission reports, the emphasis should be on bias reduction. Consequently, we would be better off using a value for γ_0 which is somewhat too large rather than one which is too small. A better approach could be to introduce a hierarchical model and use a hyperprior for

γ_0. This may be done within the current framework by multiplying the posterior (4) by a prior $p(\gamma_0)$ and computing the (global) posterior mode with respect to $(\boldsymbol{\beta}, \sigma^2, a, \gamma_0)$. Alternatively, an Empirical Bayes approach could be used.

The precision of our estimates depends on the locations of monitoring stations. In general, increasing the number of monitoring stations will give better emissions estimates. In Section 2, we argued that locating monitoring stations near large emission sources may introduce bias in emissions estimates. Furthermore, the detailed geometry of the monitoring network affects the variance of emissions estimates in a non-trivial manner through interaction with the EMEP model coefficients. Although beyond the scope of this paper, the problem of locating new monitoring stations can be addressed by the current framework. In particular, we may quantify the effect of adding or deleting monitoring stations on the estimates of emissions from various regions. This is in contrast to the problem commonly considered in spatial sampling design, where optimal sampling is usually related to optimal prediction (Cressie 1991, pp. 313–337).

Another question is the sensitivity of our results to possible systematic errors in the EMEP model. Such EMEP model errors may be assessed by applying this statistical method to data of other acidifying air pollutants. Other questions on sensitivity include alternative regional subdivisions. Stochastic

simulation may prove a useful tool for addressing these and related topics.

Our framework can also be used for enhancing the EMEP predicted sulphate concentrations and depositions. In general, one should expect better correspondence between predicted and measured concentrations when using the proposed method than when using reported emissions only. This has bearing also on predicting exceedances of critical loads, and is another topic for further research.

Even though statistical interpolation of the residuals may further improve predictions, only posterior predicted concentrations can be attributed to regional sources, through the link provided by the EMEP model. In this context, the residual field is a nuisance term representing unexplained variability, i.e. sulphate not accounted for by the EMEP model. The proposed framework is a tool for reducing the importance of the unexplained variability relative to the explained variability. This would be preferable for decision making, since only the explained variability is subject to negotiations on emissions reductions.

In the future, the current procedure for parameter estimation could be compared with a Markov Chain Monte Carlo (MCMC) approach. This would give the complete 48-dimensional joint distribution of the emissions. In practise, however, one may be content with summary statistics (mean and standard

deviation) such as presented here.

Further work should also include extending the method to include other monitored sulphur compounds, such as sulphur dioxide and particulate sulphate. This may enhance predictions of total depositions and would modify predicted exceedances of critical loads. Emissions estimates may be further improved by including data from several years, although a more elaborate statistical model would be required to incorporate possible temporal correlations. To this date, all data should be available for estimating compliance with the Helsinki protocol on 30% reduction of sulphur dioxide emissions. In the future, we hope to use the method for investigating compliance with the Oslo Protocol, and to extend the method to include nitrogen and volatile organic compounds.

Acknowledgements

This research was supported in part by the Research Council of Norway, program no. STP 28402. The author is grateful to three anonymous referees for valuable comments. The author is also indebted to Erik Berge and Magne Aldrin for helpful discussions. Hilde Sandnes and Helge Styve of the Norwegian Meteorological Institute are thanked for providing model results and emissions data. The author is also grateful to the Norwegian Institute of Air Research for providing the monitoring data. Finally, I thank Tove Andersen and Turid Follestad of the Norwegian Computing Center for some useful software subroutines.

References

Barrett, K., Seland, Ø., S., M., Sandnes, H., Styve, H. & Tarrasón, L. (1995), European transboundary acidifying air pollution: Ten years calculated fields and budgets to the end of the first sulphur protocol, EMEP/MSC-W Report 1/95, The Norwegian Meteorological Institute, Oslo, Norway.

Berger, J. O. (1985), *Statistical Decision Theory and Bayesian Analysis*, Springer Verlag, New York.

Box, G. E. P. & Tiao, G. C. (1973), *Bayesian Inference in Statistical Analysis*, Addison Wesley Publishing Company, London.

Dempster, A. P., Laird, N. & Rubin, D. B. (1977), 'Maximum likelihood from incomplete data via the EM algoritm', *Journal of Royal Statistical Society, Series B* **39**, 1–38.

Gilks, W. R., Richardson, S. & Spiegelhalter, D. J. (1996), *Markov Chain Monte Carlo in Practice*, Chapman and Hall, London.

Handcock, M. S. & Stein, M. L. (1993), 'A Bayesian analysis of Kriging', *Technometrics* **35**, 403–410.

Handcock, M. S. & Wallis, J. R. (1994), 'An approach to statistical spatial-temporal modeling of meteorological fields', *Journal of the American Statistical Association* **89**(426), 368–378.

Hjort, N. L. & Omre, H. (1994), 'Topics in spatial statistics', *Scandinavian Journal of Statistics* **21**(4), 289–357. With discussion.

Kitanidis, P. K. (1986), 'Parameter uncertainty in estimation of spatial functions: Bayesian analysis', *Water Resources Research* **22**(4), 499–507.

Le, N. D. & Zidek, J. V. (1992), 'Interpolation with uncertain spatial covariances: A Bayesian approach to Kriging', *Journal of Multivariate Analysis* **43**, 351–374.

Louis, T. A. (1982), 'Finding observed information using the EM algoritm', *Journal of Royal Statistical Society, Series B* **44**, 98–130.

Mardia, K. V. & Marshall, R. J. (1984), 'Maximum likelihood estimation of models for residual covariance in spatial regression', *Biometrika* **71**, 135–146.

Mardia, K. V. & Watkins, A. J. (1989), 'On the multimodality of the likelihood in the spatial linear model', *Biometrika* **76**, 289–295.

Omre, H. (1987), 'Bayesian Kriging – merging observations and qualified guesses in Kriging', *Mathematical Geology* **19**, 25–39.

Omre, H. & Halvorsen, K. (1989), 'The Bayesian bridge between simple and universal Kriging', *Mathematical Geology* **21**, 767–786.

Pilz, J. (1991), *Bayesian Estimation and Experimental Design in Linear Regression Models*, Wiley, New York.

Schaug, J., Pedersen, U. & Skjelmoen, J. E. (1992), Data report 1990. Part 1: Annual summaries, EMEP/CCC–Report 2/92, NILU, Lillestrøm, Norway.

Schaug, J., Pedersen, U., Skjelmoen, J. E. & Kvalvågnes, I. (1992), Data report 1990. Part 2: Monthly and seasonal summaries, EMEP/CCC–Report 3/92, NILU, Lillestrøm, Norway.

Tanner, M. A. (1993), *Tools for Statistical Inference*, Springer series in statistics, 2. edn, Springer Verlag Inc., New York.

Warnes, J. J. & Ripley, B. D. (1987), 'Problems with likelihood estimation of covariance functions of spatial Gaussian processes', *Biometrika* **74**, 640–642.

Biographical Sketch

Gudmund Høst is a Senior Research Scientist at Norwegian Computing Center, Oslo, Norway. His main interests are spatial and spatial-temporal statistics, and their applications to environmental data. Current research include air pollution monitoring, meteorology and flood forecasting. Dr Høst has also worked with marine fisheries, whale stocks and oceanography. He received his M.S. in fluid mechanics and his Ph.D. in statistics from the University of Oslo.

Code	Region	Prior	Posterior	Increase	Rel. Change	CV
AL	Albania	120	120	0	1.00	0.30
AT	Austria	90	91	1	1.01	0.30
BE	Belgium	317	317	0	1.00	0.30
BG	Bulgaria	2020	2030	10	1.01	0.30
DK	Denmark	180	187	7	1.04	0.29
FI	Finland	260	273	13	1.05	0.28
FR	France	1298	1281	-17	0.99	0.28
DD	German Dem. Rep.	4755	4545	-210	0.96	0.28
DE	Germany,Fed. Rep.	878	885	7	1.01	0.29
GR	Greece	510	511	1	1.00	0.30
HU	Hungary	1010	1079	69	1.07	0.28
IS	Iceland	6	6	0	1.00	0.30
IE	Ireland	178	178	0	1.00	0.30
IT	Italy	2251	2715	464	1.21	0.24
LU	Luxembourg	16	16	0	0.99	0.30
NL	Netherlands	201	205	4	1.02	0.29
NO	Norway	54	54	0	1.00	0.30
PL	Poland	3210	3111	-99	0.97	0.21
PT	Portugal	282	282	0	1.00	0.30
RO	Romania	1504	1523	19	1.01	0.30
ES	Spain	2316	2336	20	1.01	0.30
SE	Sweden	130	132	2	1.02	0.29
CH	Switzerland	62	63	1	1.01	0.30
TR	Turkey	354	354	0	1.00	0.30
GB	United Kingdom	3760	4206	446	1.12	0.21
REM	Remaining Areas	813	817	4	1.00	0.30
BAS	Baltic Sea	72	73	1	1.01	0.30
NOS	North Sea	174	176	2	1.01	0.30
ATL	North East Atlantic Ocean	316	317	1	1.01	0.30
MED	Mediterranean Sea	12	12	0	1.00	0.30
NAT	Natural Oceanic	721	733	12	1.02	0.29
RU1	Kola/Karelia	759	766	7	1.01	0.30
RU2	Leningrad/Novgorod-Pskov	317	321	4	1.01	0.30
RU3	Kaliningrad	44	45	1	1.01	0.30
BY	Belarus	710	726	16	1.02	0.29
UA	Ukraine	3850	3904	54	1.01	0.30
MD	Reublic of Moldova	91	91	0	1.00	0.30
RU4	Rest of Russia	3339	3362	23	1.01	0.30
EE	Estonia	240	244	4	1.02	0.29
LV	Latvia	82	82	0	1.00	0.30
LT	Lithuania	136	138	2	1.02	0.30
CS*	Czech Republic	1876	1822	-54	0.97	0.30
SK	Slovakia	543	557	14	1.03	0.29
SI	Slovenia	195	218	23	1.12	0.26
HR	Croatia	180	184	4	1.02	0.29
BA	Bosnia-Hercegovina	480	529	49	1.10	0.27
YU*1	F.Yugoslavia (-SI,HR,BA,YU*1)	508	513	5	1.01	0.30
YU*2	FYR Macedonia	10	10	0	1.00	0.30
	Total	41228	42140	912	1.02	-

Table 1: *Results of emissions estimation. Prior Emission, Posterior Estimated Emission and Increase are in units of 1000 tons of sulphur dioxide*

Grid block ID	Prior	Posterior	Increase	Rel. Change	Measured
AT4	0.55	0.56	0.004	1.01	0.59
BE1	0.69	0.69	0.003	1.00	0.96
CH1	0.21	0.22	0.007	1.03	0.34
DE1	0.61	0.66	0.050	1.08	0.77
DE3	0.46	0.46	-0.004	0.99	0.54
DE4	0.65	0.65	0.001	1.00	0.69
DE5	0.89	0.88	-0.011	0.99	0.85
DK5	0.68	0.72	0.034	1.05	1.13
FR3	0.26	0.26	0.002	1.01	0.42
FR9	0.69	0.69	0.003	1.00	0.61
FR11	0.30	0.30	0.000	1.00	0.47
IT5	0.46	0.48	0.026	1.06	0.95
IE1	0.02	0.02	0.000	1.02	0.27
IS2	0.04	0.04	0.002	1.04	0.22
NO1	0.35	0.38	0.027	1.08	0.71
NO8	0.42	0.46	0.039	1.09	0.39
NO15	0.07	0.07	0.004	1.05	0.16
NO39	0.07	0.08	0.005	1.06	0.11
NO41	0.28	0.29	0.010	1.04	0.55
NL8	1.06	1.14	0.081	1.08	1.31
PL1	1.04	1.03	-0.011	0.99	1.53
SE2	0.47	0.50	0.022	1.05	0.98
SE5	0.08	0.08	0.004	1.05	0.53
SE8	0.60	0.61	0.004	1.01	1.23
SE11	0.72	0.74	0.023	1.03	1.22
SE12	0.37	0.38	0.009	1.02	0.84
SE13	0.11	0.12	0.001	1.01	0.30
FI4	0.25	0.26	0.005	1.02	0.43
FI17	0.40	0.40	0.007	1.02	0.98
FI22	0.27	0.28	0.003	1.01	0.38
SU3	0.85	0.85	0.002	1.00	0.77
SU4	1.82	1.78	-0.036	0.98	1.63
SU5	1.82	1.78	-0.036	0.98	1.67
SU6	1.84	1.81	-0.033	0.98	1.92
SU9	0.50	0.51	0.008	1.02	0.76
SU10	0.85	0.85	0.002	1.00	0.87
GB2	0.22	0.24	0.021	1.09	0.45
GB6	0.09	0.09	0.002	1.02	0.23
GB13	0.20	0.22	0.013	1.06	0.32
YU2	0.57	0.63	0.062	1.11	1.31
YU4	0.59	0.64	0.042	1.07	1.16
YU6	0.59	0.64	0.046	1.08	1.36

Table 2: *Predicted concentrations at the monitoring stations (See Figure 1) included in the study. Prior predicted concentrations, Posterior (based on estimated emissions) predicted concentrations and Increase are in units of mg(S)/l*

Emitter	Prior coefficient of variation				
	0	0.2	0.3	0.5	1
DD	**2377**	2378	2391	2517	2632
IT	2251	2436	2671	3453	5011
PL	3210	3260	3308	3406	3295
GB	3760	3910	4063	4506	4680
DD	**4755**	4617	4545	4682	4332
IT	2251	2455	2715	3587	5300
PL	3210	3131	3111	3086	3009
GB	3760	3991	4206	4753	4898
DD	**9510**	7865	7115	6601	5519
IT	2251	2471	2755	3694	5433
PL	3210	2863	2793	2736	2801
GB	3760	4073	4345	4937	5166

Table 3: *Posterior estimated emissions for various prior specifications, in units of 1000 tons of sulphur dioxide. Boldface numbers indicate hypothetical reported emission from former German Democratic Republic (DD)*

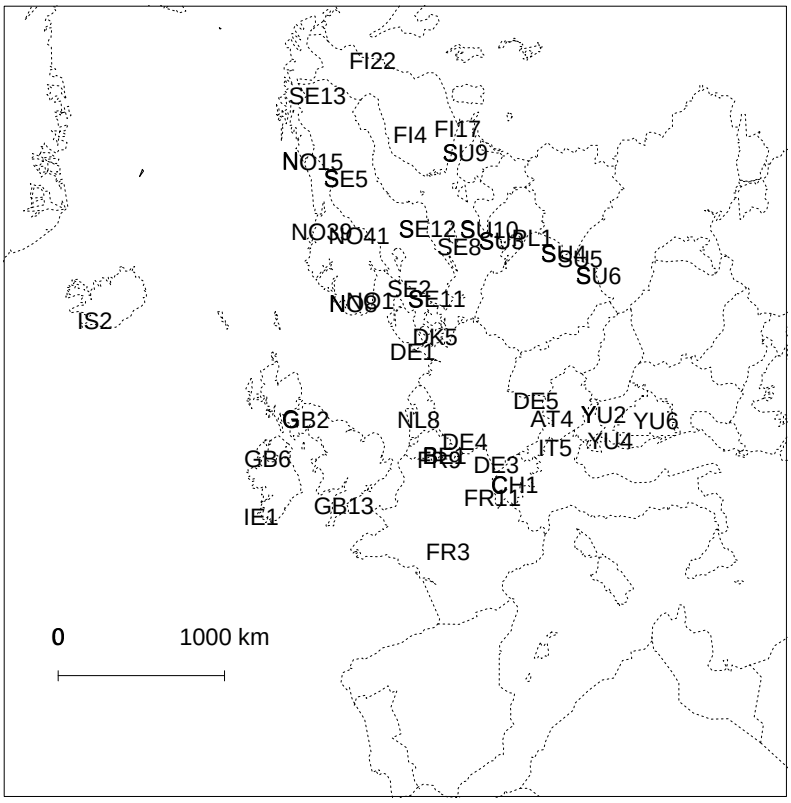

Figure 1: *Study area and data locations. Concentrations at the monitoring stations are given in Table 2*

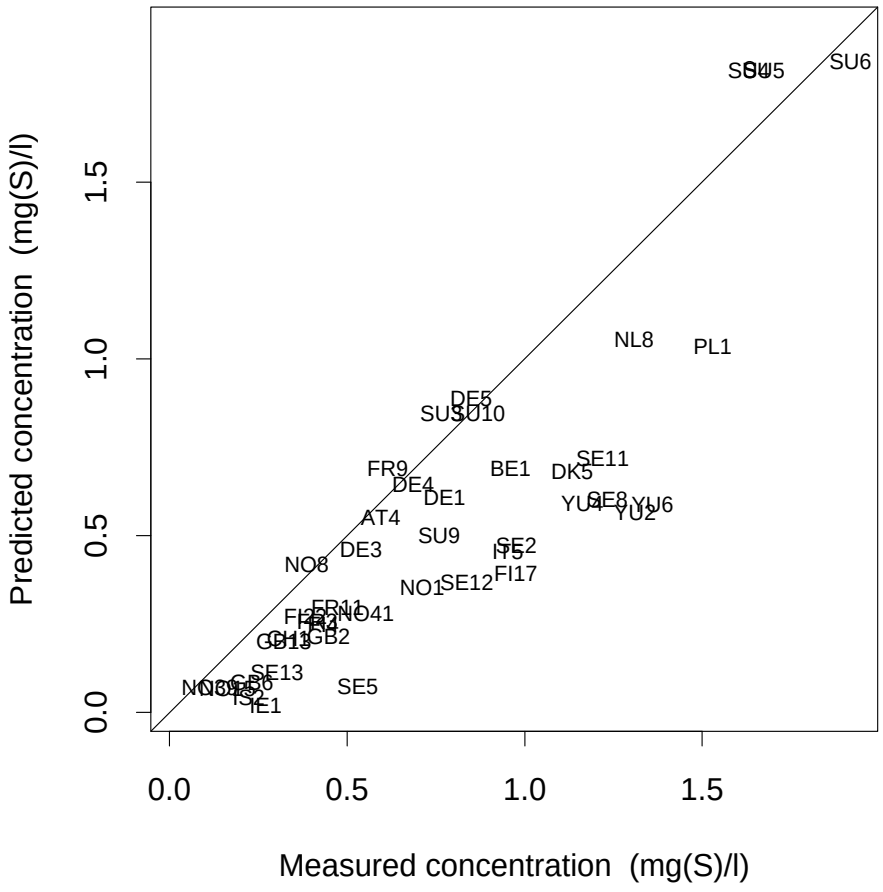

Figure 2: *Average concentration of sulphate in precipitation in 1990 as measured by monitoring stations and corresponding prior prediction from the EMEP model*

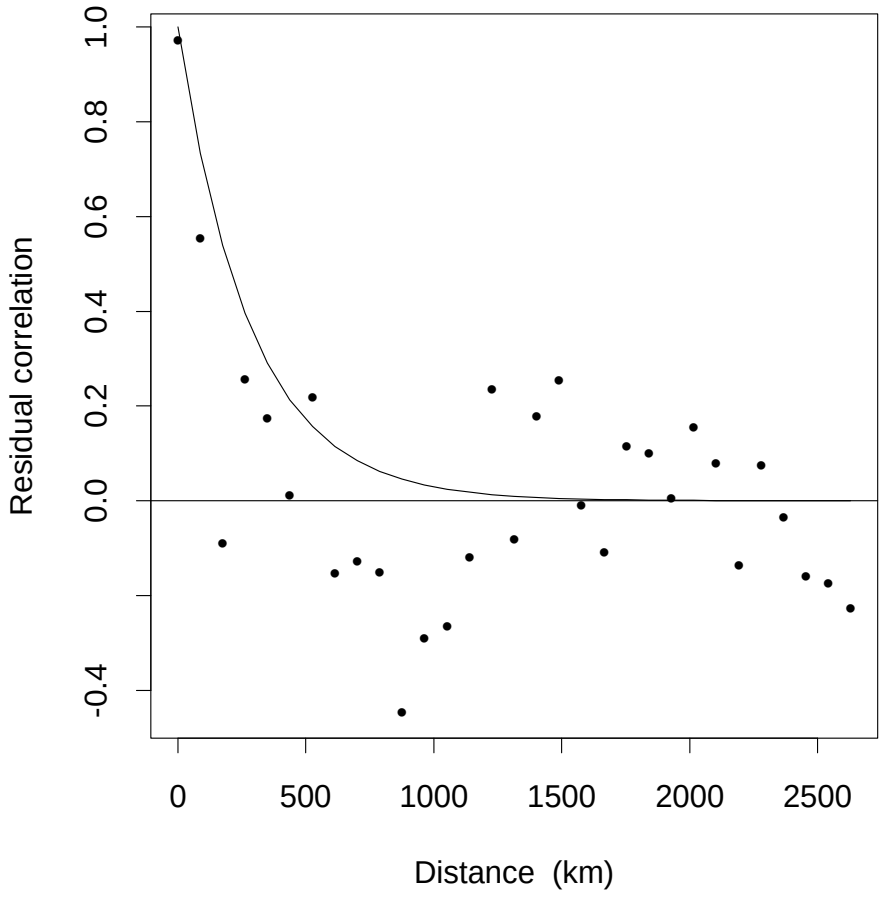

Figure 3: *Correlogram of fitted residuals (points) and estimated correlation function (line) with range=851 km*

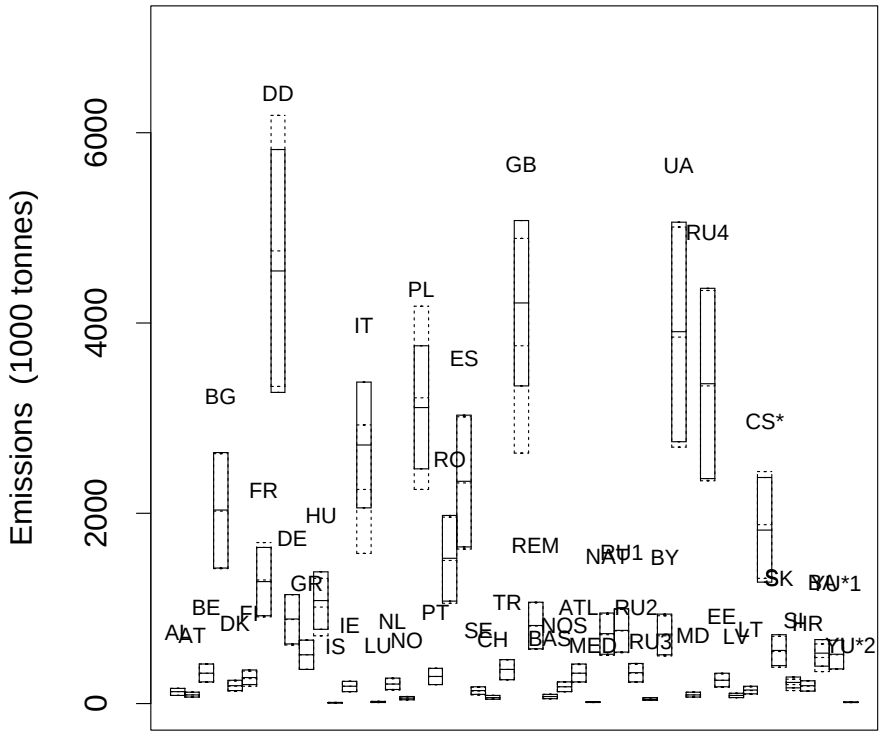

Figure 4: *Posterior estimated emissions (full boxes) and prior emissions (broken boxes) for each region. Predicted emission and ± one (estimated) standard deviation. Region codes are explained in Table 1*

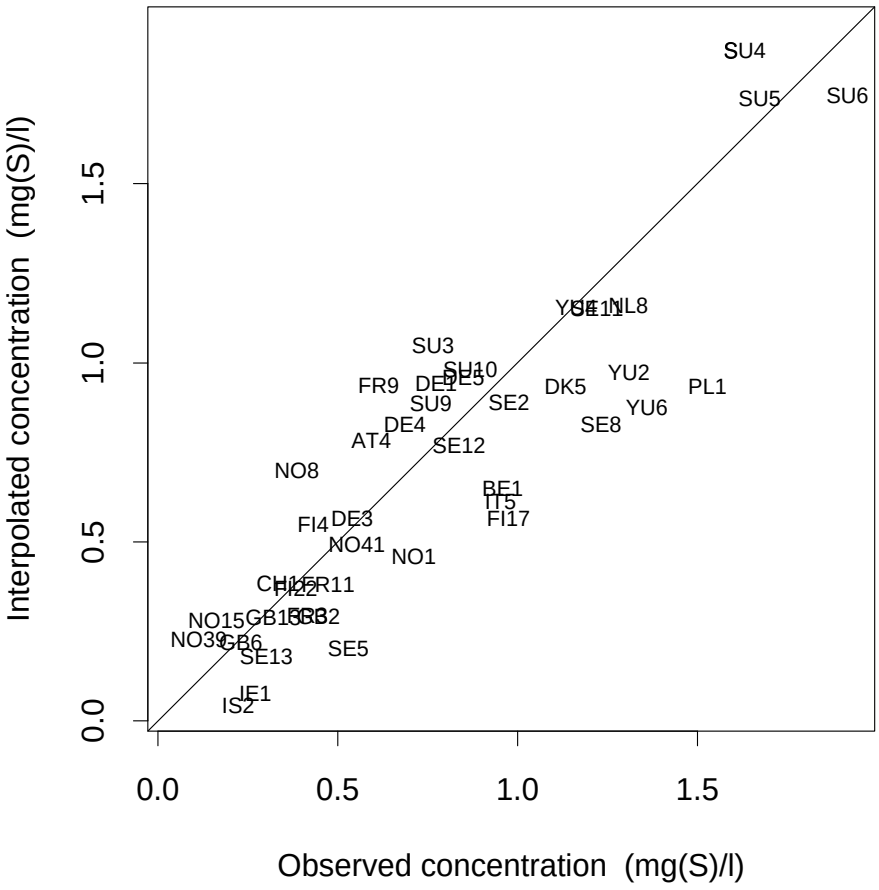

Figure 5: *Observed versus cross-validated sulphate concentrations at monitoring stations. See Figure 1 for location of monitoring stations*